ALMA MATER STUDIORUM
UNIVERSITÀ DI BOLOGNA

ARCHIVIO ISTITUZIONALE
DELLA RICERCA

Alma Mater Studiorum Università di Bologna
Archivio istituzionale della ricerca

Wearable, Energy-Autonomous RF Microwave Systems

This is the final peer-reviewed author's accepted manuscript (postprint) of the following publication:

Published Version:
Costanzo A., Benassi F., Monti G. (2022). Wearable, Energy-Autonomous RF Microwave Systems. IEEE MICROWAVE MAGAZINE, 23(3), 24-38 [10.1109/MMM.2021.3130708].

Availability:
This version is available at: https://hdl.handle.net/11585/863819 since: 2024-03-01

Published:
DOI: http://doi.org/10.1109/MMM.2021.3130708

Terms of use:

Some rights reserved. The terms and conditions for the reuse of this version of the manuscript are specified in the publishing policy. For all terms of use and more information see the publisher's website.

This item was downloaded from IRIS Università di Bologna (https://cris.unibo.it/).
When citing, please refer to the published version.

(Article begins on next page)

07 November 2024

Wearable energy autonomous RF microwave systems

Alessandra Costanzo, Francesca Benassi, Giuseppina Monti

Alessandra Costanzo (alessandra.costanzo@unibo.it) and Francesca Benassi (francesca.benassi9@unibo.it) are with Alma Mater Studiorum - University of Bologna, DEI - Department of Electrical, Electronic and Information Engineering "Guglielmo Marconi", Bologna, Italy. Giuseppina Monti (giuseppina.monti@unisalento.it) is with University of Salento, DII- Department of Engineering for Innovation, Lecce, Italy

.

Abstract: In the next future we will be surrounded in our daily lives by a multitude of small, relatively inexpensive computing devices, equipped with wireless communication and sensing featuring the concept of "pervasive intelligence", a basis from which we can envision our future world as an Internet of Everything (IoT/IoE), in terms of both a consumer IoT/IoE and the Industrial IoT. Indeed IoT is a technological paradigm with boundless application potentials and it is increasingly becoming a reality able to improve the competitiveness of businesses, the efficiency of public administrations and the quality of life.

Over the last few years, numerous IoT-inspired systems have been developed and the applied fields have expanded and profoundly evolved: smart home, smart building, smart metering, smart factory, smart cars, smart city, and so on with smart environment, smart agriculture, smart logistics, smart lifecycle, smart retail and smart health. One of the key desired characteristics of an IoT wireless sensor node is its capability to operate autonomously from energy harvesting (EH) rather than relying on bulky batteries, which have a limited lifetime. Furthermore, for many of the above-mentioned scenarios, wearable solutions are foreseen to further increase the pervasive diffusion of the IoT paradigm, enabling a multitude of devices and individuals connected to each other.

The keywords for the development of successful RF autonomous systems, possibly wearable, are the following:

- non-intrusiveness: users must be able to carry out their activities without limitation caused by the wireless device;
- seamless integration with wearable accessories and clothes;
- sensing and localization: the device must be localized and equipped with one or more sensors; wireless connectivity, by means of ultra-low power solutions;
- energy autonomy: the device must guarantee a long energy autonomy, possibly over its lifetime.
- human-centered design: fundamental for the success of wearable devices, whose main purpose should be to optimize the user experience.

Non-intrusiveness and seamless integration into wearable accessories and garments, require creative manufacturing techniques and unconventional materials, such as flexible ones, to adapt to the soft curves of a human body or an object or textiles able to integrate the IoT devices into clothing, subjected to washing and ironing operations. [1]. Another strategy is to develop devices that can be applied directly to the skin like patches, the so-called "epidermal electronics"[2]-[5].

© 2022 IEEE. Personal use of this material is permitted. Permission from IEEE must be obtained for all other uses, in any current or future media, including reprinting/republishing this material for advertising or promotional purposes, creating new collective works, for resale or redistribution to servers or lists, or reuse of any copyrighted component of this work in other works.

Energy-autonomy is certainly a fundamental enabling technology for the IoT paradigm, and it is currently demonstrated by many RF wireless systems based on either fully passive devices or active ones, exploiting "on-demand" wireless power transfer or energy scavenging technologies.

For passive wireless systems, an attractive solution is the chip-less technology, that has been firstly exploited for radio-frequency identification (RFID). Recently it has been demonstrated for sensing and localization purposes with a high level of integrability into wearable garments or accessories. Indeed the absence of chips and electronic components makes this approach particularly suitable for being integrated into garments, using conductive textile materials (threads or fabrics), thus resulting in devices that can be washed and ironed.

As per energy autonomous devices, based on WPT or energy harvesting, can include chips or electronic circuitry not only for RF-to-DC conversion purposes but also for implementing sensing and localization activities.

In this paper an overview of some recently proposed energy autonomous wearable devices exploiting, both the approaches describe above are presented. The emphasis will be dedicated, but not limited to, devices fabricated using textile or flexible materials.

Electromagnetic-Based Energy Harvesting systems

The first topologies of RF passive systems that are described in this work are based on Electromagnetic energy harvesting. The systems are derived both on substrates dedicated to RF applications, to achieve good performance even in the presence of low received power, but also on daily-use materials such as paper or even clothes [6].

Although the presented works describe innovative implementations that contribute to make each of them unique, the common thread remains the presence of a circuitry, which can either be a simple chip, as in RFID devices, or a customized implementation, exploiting microstrip technology [7]. As anticipated in the introduction, many are fields in which devices powered by energy harvesting can find suitable applications, as it is described in the following.

Harmonic Tag

Exploiting harmonic power harvesting has been found to be an interesting technique to be applied within RFID sensor tags applications [8],[9]. These tags are not exploited for identification purposes only, but they can also be equipped with sensors to perform a more thorough analysis of the environment in which they are located [10-12]. The basic operating principles rely on the generation of a backscattered signal at one or more higher harmonics with respect to the received one. This principle has been exploited to overcome some issues related to RFID system which may be vulnerable to clutter noise or self-jamming during multiple reader setup [13]

In [14], a paper-based harmonic tag transponder is presented. The antenna is designed as an annular slot antenna tuned to receive an RF signal transmitted by the reader at the fundamental frequency f_0 of 1.2 GHz and transmit a $2f_0$ signal generated by a frequency multiplier. A schematic representation of the system is reported in Figs.1, together with the photo of the prototype.

© 2022 IEEE. Personal use of this material is permitted. Permission from IEEE must be obtained for all other uses, in any current or future media, including reprinting/republishing this material for advertising or promotional purposes, creating new collective works, for resale or redistribution to servers or lists, or reuse of any copyrighted component of this work in other works.

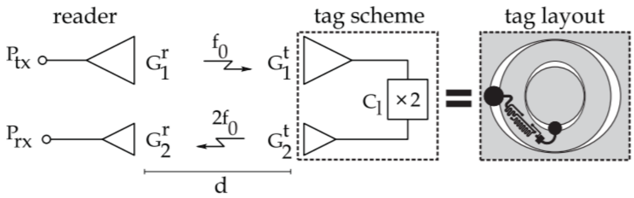

(a)

(b)

Fig.1 (a) Schematic description of the harmonic tag. (b) photo of the front and back view of the prototype [14]

The antenna is designed by means of full-wave simulations and performs good matching for both the operating frequencies, experiencing a -10dBm fractional bandwidth of 22% for f_0 and 12% for $2f_0$, while maintaining a good decoupling. The second harmonic is generated by means of a Schottky diode HSMS-2850 operating as a frequency doubler, connected to the antenna through a matching network. As the circuit schematic in Fig 1b shows, the two meandered quarter-wave stubs are used as harmonic filter, allowing only the fundamental frequency to flow into the diode. An LC high-pass filter on the diode output guarantees a load impedance at $2f_0$ while offering a negligible resistive component at f_0. With this design, the whole signal at f_0 is used to activate the diode, whereas a maximum power transfer to the load is guaranteed only for the $2f_0$. Experimental validations are carried out using a reader equipped with a circularly polarized antenna, to avoid degradations due to tag-reader misalignment. For a transmitted power of 11 dBm, the maximum reading range is found to be around 4 m, showing good agreement with the expected performance, as described in Fig.2, where "meas 1" and "meas 2" refer to a tag aligned to on the horizontal and vertical polarization orientation of the antenna respectively.

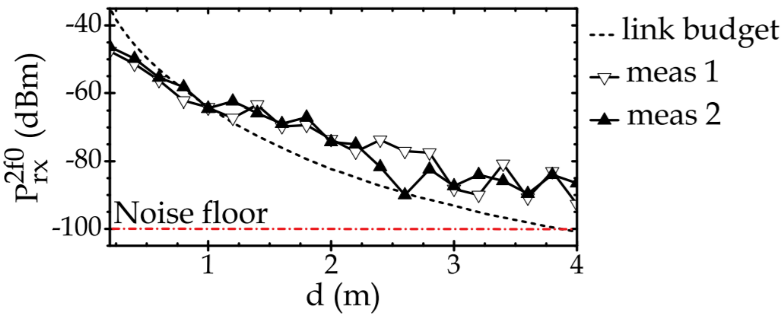

Fig.2 Measured and simulated results for the proposed system, for a 11 dBm transmitted power [14].

© 2022 IEEE. Personal use of this material is permitted. Permission from IEEE must be obtained for all other uses, in any current or future media, including reprinting/republishing this material for advertising or promotional purposes, creating new collective works, for resale or redistribution to servers or lists, or reuse of any copyrighted component of this work in other works.

The compactness and the energy autonomy of this system makes it suitable to be applied in modern IoT scenarios, fulfilling some of the most important requirements such as energy autonomy, miniaturization, and lightness.

Energy harvesting systems for localization-purposes

Indoor positioning system (IPS) is considered one the new developing technologies of these last years, and the methods adopted for its actuation are several and different; in that sense, the use of UWB (typically backscattered) signals [15] seems to be well promising because of the exploitation of a very large range of frequencies allowing to avoid possible effects of fading and shadowing that could occur with high probability in indoor environments at certain frequencies, at the same time, these procedures need reference nodes for a safe implementation of the signal processing technique to obtain centimeter-level localization. Battery-less UWB tags with on-board ultra-low power UWB pulse generator chips have been recently demonstrated for localizing objects in space [16], but similar performance can be reached with the chipless solution presented in [17], where the multi-sine excitation at UHF, normally adopted for increasing the rectifier RF-to-dc efficiency only [18], is exploited for two different goals: 1) energy harvesting, by converting energy from RF to dc and 2) passive generation of a quasi-UWB impulse by backscattering the intermodulation products of the same multi-sine excitation, that are normally filtered out and wasted. Fig. 3 represents the passive, battery-less UWB tag concept [17].

Fig. 4 shows the circuit schematic of the UWB tag: it consists of a standard rectenna designed for energy harvesting purposed at UHF (centered at 871.5 MHz), with a frequency-multiplexing output section consisting of the dc path and a UWB one which is connected to a UWB antenna radiating the IM products (in the lower UWB European bandwidth: 2 GHz – 6 GHz) generated by the rectifier itself.

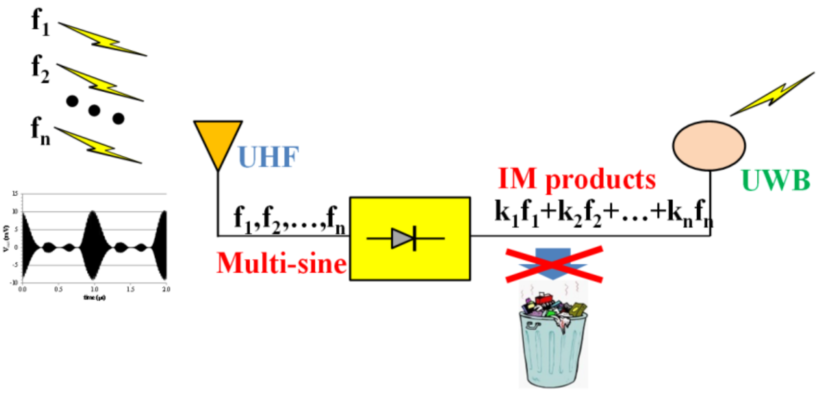

Fig.3 Passive, battery-less UWB tag concept.

© 2022 IEEE. Personal use of this material is permitted. Permission from IEEE must be obtained for all other uses, in any current or future media, including reprinting/republishing this material for advertising or promotional purposes, creating new collective works, for resale or redistribution to servers or lists, or reuse of any copyrighted component of this work in other works.

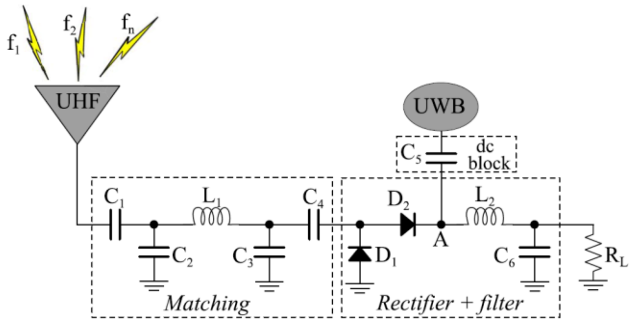

Fig.4 Circuit schematic of the UWB tag.

The presented system is interposed between a multisine UHF transmitter and multiple UWB receivers. The tag localization is performed by processing the time difference-of-arrival (TDOA) between the signal that is backscattered by the tag received by the anchor nodes. When the anchor node representing the localization receiver (Rx) is close to the tag (i.e., 1 m), the algorithm selects the 3^{rd}, 4^{th} and 5^{th} harmonics as useful components.

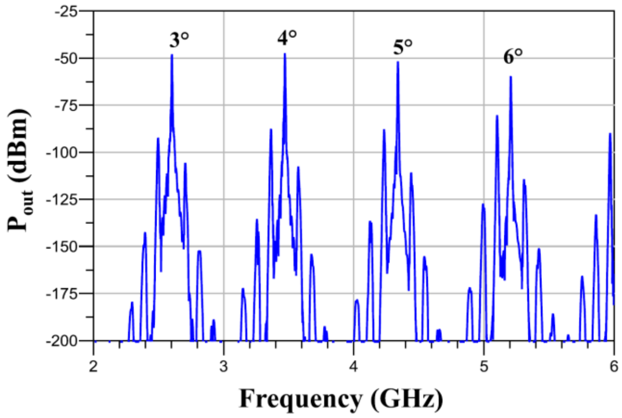

Fig. 4 Power spectrum generated by a UHF excitation made by four-tones [17].

Differently, when the tag is farther (i.e., 4 m), the 5^{th} harmonic is discarded since it is too much corrupted by noise. With the smaller bandwidth of the multisine excitation (500 kHz), a high-accuracy (error below 20 cm) can be reached up to tag-Rx distance of 8 m for an observation time T_{obs}= 200 ms, and up to 12 m for T_{obs}=500 ms, while with the larger bandwidth (2 MHz) up to 12 m and 16 m, respectively. The estimated root-mean-square error for increasing tag-RX distances in shown in Fig. 5.

© 2022 IEEE. Personal use of this material is permitted. Permission from IEEE must be obtained for all other uses, in any current or future media, including reprinting/republishing this material for advertising or promotional purposes, creating new collective works, for resale or redistribution to servers or lists, or reuse of any copyrighted component of this work in other works.

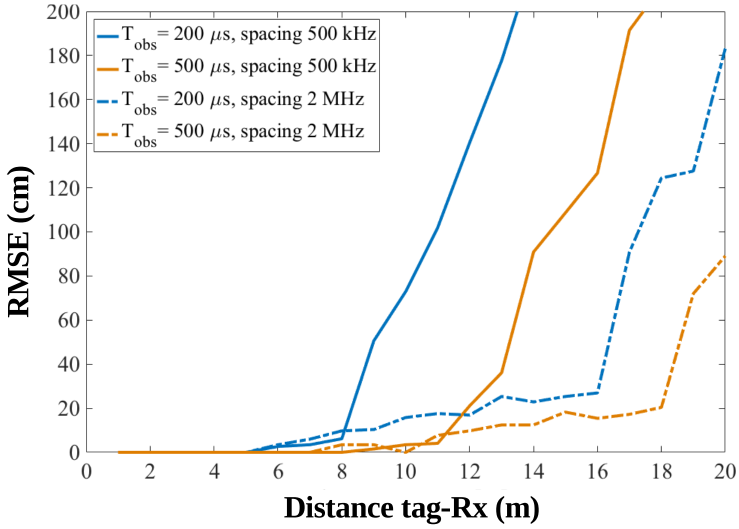

Fig. 5 RMSE estimation considering two different bandwidth, 500 KHz and 2 MHz respectively

One of the interesting aspects of this solution [17] is the implementation of the multisine excitations within the circuit simulation of the whole system, which has allowed to perform accurate circuital simulations reducing the overall requested computational time. The multitone excitations have been represented as higher harmonics of the same fundamental frequency, which corresponds to the tones spacing. With this approach, the multi-sine non-linear analysis is carried out as a single-tone analysis with a very large number of harmonics instead of a multi-tone one, thus allowing a large number of tones to be accounted for with a much faster simualtions, especially for increasing number of tones as summarized in the table of Fig. 6.

Regime	No. tones	IMD order	No. Spectral lines	CPU time (s)
Quasi-periodic	4	6	644	36
Quasi-periodic	8	4	19912	74,280
Periodic	4	-	6000	35
Periodic	8	-	12000	42
Periodic	16	-	24000	55

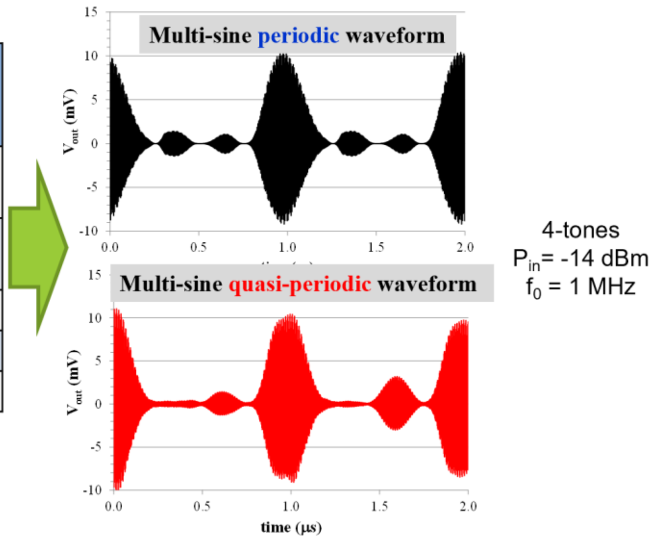

Fig. 6 Computational time requested for circuital simualtions in the case of quasi-periodic and periodic regime.

© 2022 IEEE. Personal use of this material is permitted. Permission from IEEE must be obtained for all other uses, in any current or future media, including reprinting/republishing this material for advertising or promotional purposes, creating new collective works, for resale or redistribution to servers or lists, or reuse of any copyrighted component of this work in other works.

It has been demonstrated that tones spacing is a crucial design parameter for improving the localization capabilities, the higher the tones spacing the better is the localization accuracy. Simulations have then led to optimizations aimed to quantify the number of tones and the frequency spacing Δf to be used to obtain the highest harmonic content.
As it can be noticed from the plots of Figs. 7 an enlargement of the harmonic content can be achieved by increasing the frequency spacing Δf.

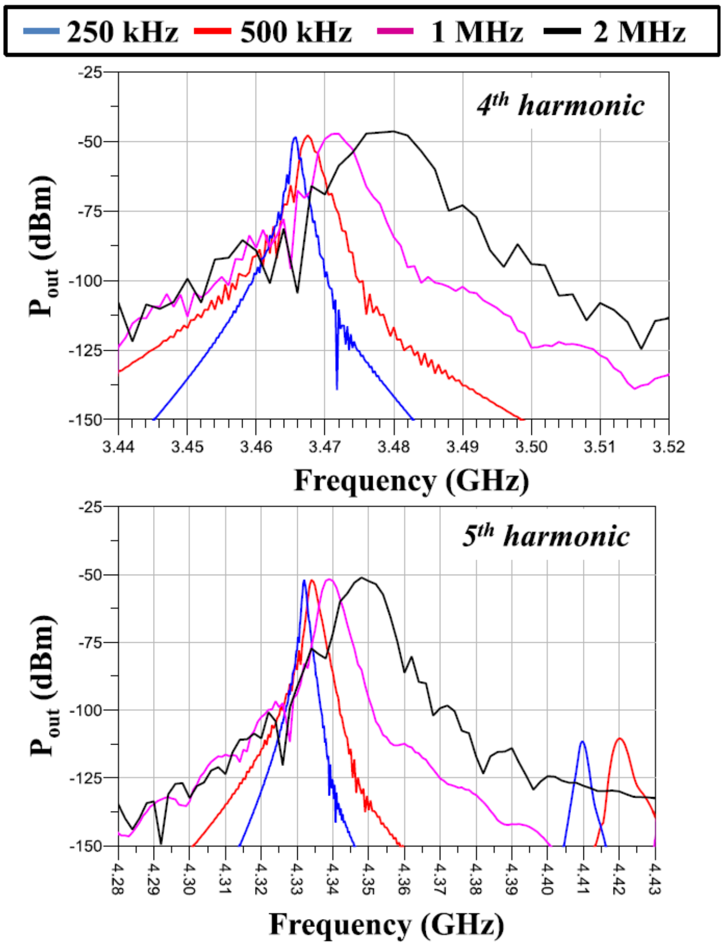

Fig.7 Power spectral line for the fourth and fifth harmonic for the UHF signal when the frequency spacing is increased [17].

Passive sensing by exploiting wearable RF energy harvesting.

Another field in which energy harvesting techniques are implemented, which is raising more and more interest nowadays, is the wearable one related to the biomedical environment. The advanced technology in the biomedical sector has led to the realization of an enormous number of wearable sensors for real-time monitoring [19] and identification of patients inside the hospital environments [20] or remotely. Having wireless technologies largely accessible has allowed to identify multiple available RF power sources that can be exploited to power sensors both in indoor and outdoor environments. In [21] a low-power passive tag performing pervasive monitoring of patient's vital parameters such as the phonocardiogram (PCG) is

© 2022 IEEE. Personal use of this material is permitted. Permission from IEEE must be obtained for all other uses, in any current or future media, including reprinting/republishing this material for advertising or promotional purposes, creating new collective works, for resale or redistribution to servers or lists, or reuse of any copyrighted component of this work in other works.

implemented, and wirelessly powered. A schematic description is reported in Fig. 8. The system is able to read multiple-sensor information and generates alarms, in case of patient emergency.

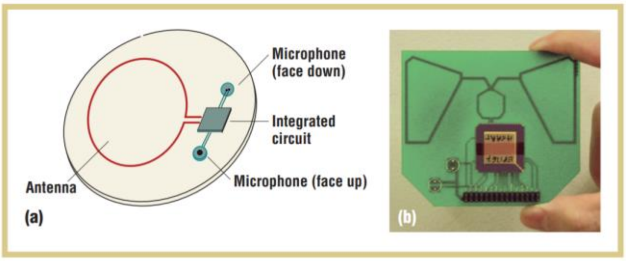

(a)

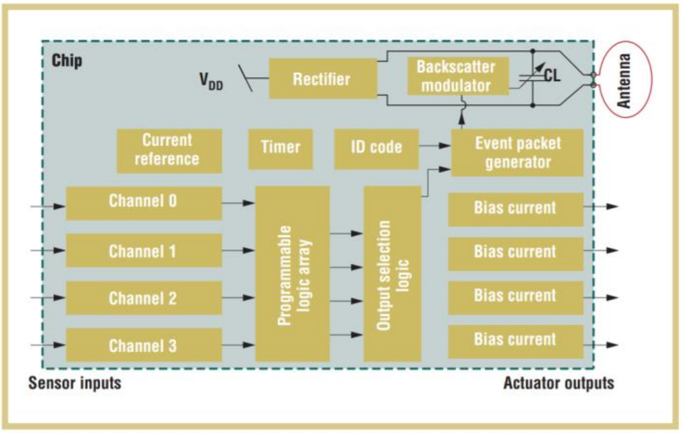

(b)

Fig. 8 (a) Pictorial representation of the RF passive tag and (b) block diagram of the chip [21].

(a)

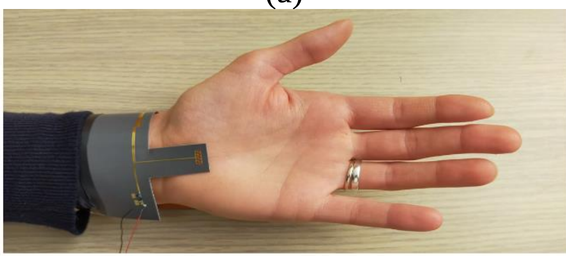

(b)

Fig. 9 Photo of the proposed energy autonomous system (a) patch antenna dedicated to the energy harvesting and (b) stub embedding the microfluidic and rectifier circuitry [25].

© 2022 IEEE. Personal use of this material is permitted. Permission from IEEE must be obtained for all other uses, in any current or future media, including reprinting/republishing this material for advertising or promotional purposes, creating new collective works, for resale or redistribution to servers or lists, or reuse of any copyrighted component of this work in other works.

The system is powered by an external transmitter operating at 900 MHz and transferring 4W of equivalent isotropic radiated power (EIRP). The available power is estimated for increasing distances of the tag from the transmitting antenna, showing that the operating range is limited to 3 m for the 2.4 GHz operating frequency, and to 12 m for the 900 MHz one. Experimental validations have shown a $15-\mu W$ output power for an operating distance of 1.3 m from the TX antenna transmitting 800 mW EIRP at 800 MHz; with an increased TX power the operating distance can be extended up to 7 m. A small microphone for the PCG has been used as primary actuator and the 15 μW received power is sufficient to run both the chip and the microphone at a bias current of 30 μA at the 1.3 m distance. Data are sent from the tag to the base station through backscatter modulation, allowing the tag to operate in low-power condition and thus being a suitable system to be powered wirelessly.

Energy harvesting can also be implied to power wearable devices dedicated to the detection of specific fluids or material. In [22] an energy autonomous filtering antenna (filtenna) operating at 2.45 GHz is used to perform a wireless detection of the presence of ethanol solution on the hand surface, for checking the correct hand sanitizing procedures.

The entire system is derived on a Rogers substrate RT/Duroid 5880, whose flexibility and thickness make it suitable for wearable applications, as shown in Fig. 9. The sensing area consists of a microstrip open stub embedding a microfluidic channel at its open end; the stub is tuned to resonate at 2.45 GHz operating frequency when a given target ethanol solution is filling the channel. When any other fluid is present the stub is detuned. To enhance frequency selectivity, the stub is placed in substitution of one open end of a 2- section coupled line filter allowing the systems to act as a selective detector only in the presence of that specific ethanol solution made of 70% ethanol and 30% water. The power received by the system patch antenna activated the sensing and it is then transduced by a rectifier circuit and read as different dc-output voltage levels. The detector, which can be worn as a bracelet is fully activated by an external 2.45 GHz-RF source avoiding the need for batteries and the system readout for different levels of received power is depicted in Fig.10 .

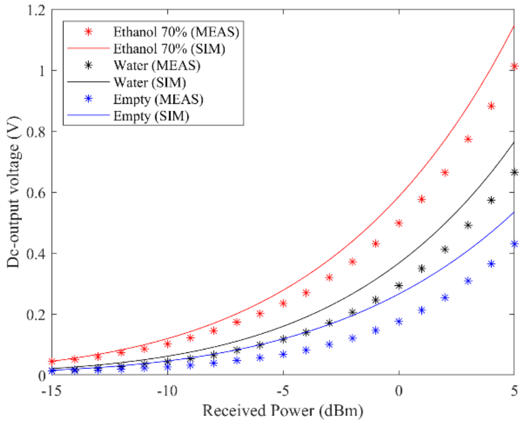

Fig. 10. Dc-output voltage levels for different received power in the presence of different fluids filling the channel [22].

© 2022 IEEE. Personal use of this material is permitted. Permission from IEEE must be obtained for all other uses, in any current or future media, including reprinting/republishing this material for advertising or promotional purposes, creating new collective works, for resale or redistribution to servers or lists, or reuse of any copyrighted component of this work in other works.

CHIPLESS

RFID chipless technology is an attractive technological solution for developing passive sensors and devices that can be seamlessly integrated into wearable accessories and clothes.

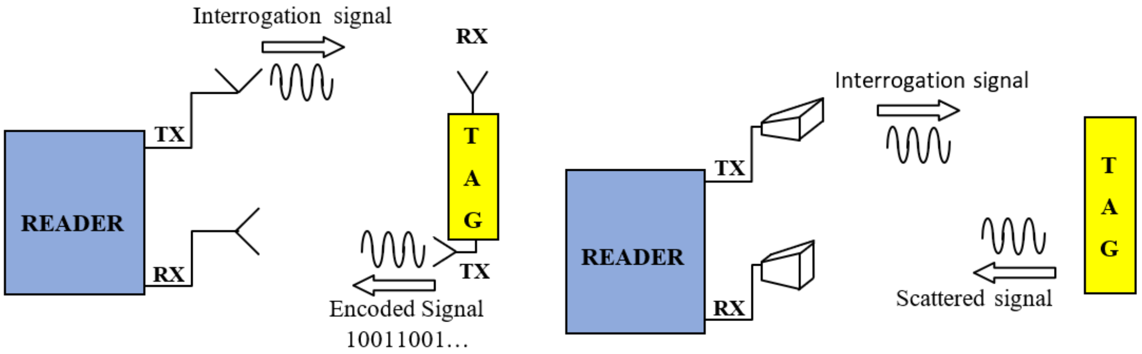

(a) (b)

Figure 11: Possible architectures of a chipless RFID system. (a) The reader and the tag are equipped with two cross-polarized antennas. (b) The tag consists of a reflective frequency selective surface.

Chipless sensors provide various advantages such as potentially infinite service-life, low-cost, low environmental impact, and robust performance in harsh scenarios, where integrated circuits (IC) could be damaged [23]-[27].
The general architecture and working mechanism of chipless RFID are the same of all RFID systems: a Reader is wirelessly connected to one or more tags. The reader is the interrogator and data collector: it transmits an RF signal and receives back the sensed data in the form of a signal scattered by the tag. The collected data are processed by the reader [28]-[30].
However, with respect to chipped tags, in chipless tags the decoding of the identifier (or that of the sensed data) is completely different. In chipless RFID, there is no communication protocol. The tag is a completely passive device and does not contain any electronic circuitry or chip, it does not embed any power recovery system or transceiver. The decoding of the data takes place exclusively from the analysis of the signal (phase and amplitude) scattered by the tag.

In this regard, different encoding techniques have been proposed in the literature for chipless RFID. Depending on the domain (frequency or time) adopted for the analysis of the scattered

© 2022 IEEE. Personal use of this material is permitted. Permission from IEEE must be obtained for all other uses, in any current or future media, including reprinting/republishing this material for advertising or promotional purposes, creating new collective works, for resale or redistribution to servers or lists, or reuse of any copyrighted component of this work in other works.

signal, two main categories can be identified: time domain reflectometry (TDR)-based tags and spectral signature-based tags [30].

In TDR-based systems [31], the information is encoded in the time domain; they are mostly based on surface acoustic wave (SAW) technology and exploit an electro-acoustic transducer connected to an antenna as tag.

In spectral signature-based systems the data is encoded in the frequency domain, they are mostly based on resonant structures and the sensed data is encoded by the presence/absence of resonance peaks in the signal scattered by the tag. As illustrated in Fig. 11, two different architectures can be used: 1) retransmission-based, and 2) backscattered-based.

In retransmission-based architectures, the tag and the reader are equipped with two cross-polarized antennas. In these schemes the tag consists of a two-port device that implements the codification and is connected to the two cross-polarized antennas. In backscattered-based architectures the tag consists of a reflective frequency selective surface and does not integrate any antenna, the information is decoded by analyzing the signal scattered by the tag. In both architectures, an ultra-wide band signal is used for interrogation.

With regard to wearable applications, wearable chipless tags have been proposed in [32]-[39]. In particular, in [32]-[38] chipless tags fabricated by using textile materials have been presented; while, in [39]-[40] chipless tags fabricated on a flexible substrate have been proposed.

TEXTILE CHIPLESS TAGS using conductive fabrics

As already mentioned, an effective approach for developing devices that can be integrated into clothing consists in using suitable textile materials. Some examples of fully-textile chipless tags have been presented in [32]-[38].

In [35] two textile chip-less tags to be used as touch sensors have been presented.

The two tags were fabricated by using a layer of pile as substrate (thickness equal to 0.5 mm, and relative dielectric permittivity equal to 1.18) and an adhesive non-woven conductive fabric (NWCF) for all the conductive parts. A cutting plotter was used to shape the NWCF.

The NWCF is an excellent material for the fabrication of textile devices, it has an electrical conductivity equal to 2.27 × 105 S/m and a thickness equal to 0.11 mm. Additionally, this fabric has good performance in terms of robustness with respect to washing and ironing and can be shaped by hand or by using a cutting plotter [41]-[43]. The geometry and photographs of the tags are given in Fig. 16:

The tag illustrated in Fig. 16a is a 2-bit multi-resonator chipless tag. It consists of a microstrip line having two resonators slotted on the ground plane. The number of bits that are available for encoding is determined by the number of resonators (for the analyzed tag it is equal to 2). The resonators on the ground plane introduce a zero in the transmission coefficient of the microstrip line (i.e., a minimum in the amplitude of the scattering parameter S_{21} of the microstrip line).

© 2022 IEEE. Personal use of this material is permitted. Permission from IEEE must be obtained for all other uses, in any current or future media, including reprinting/republishing this material for advertising or promotional purposes, creating new collective works, for resale or redistribution to servers or lists, or reuse of any copyrighted component of this work in other works.

By designing the resonators so that they have different and distinguishable frequencies of resonance distributed in the operating band, it is possible to associate the presence of a zero in the transmission coefficient of the microstrip line to a specific resonator.
Furthermore, a specific resonator can be "deactivated" by short-circuiting with a finger, as shown in Fig. 16e. In this way, each resonator can be used as a coding bit with two possible logic states "0" and "1". For a tag using n resonators, when the resonators are all active, the microstrip line will have n transmission zeros (all bits in the logic state "1"). By short-circuiting one resonator, the associated transmission zero disappears and the corresponding bit turns to the logic state “0” (see Fig. 16e-16f). In this way the tag can be used as a touch sensor: when a finger touches one resonator, it deactivates it and modifies its logical state from “1” to “0” (see the photograph in Fig. 16e-16f).

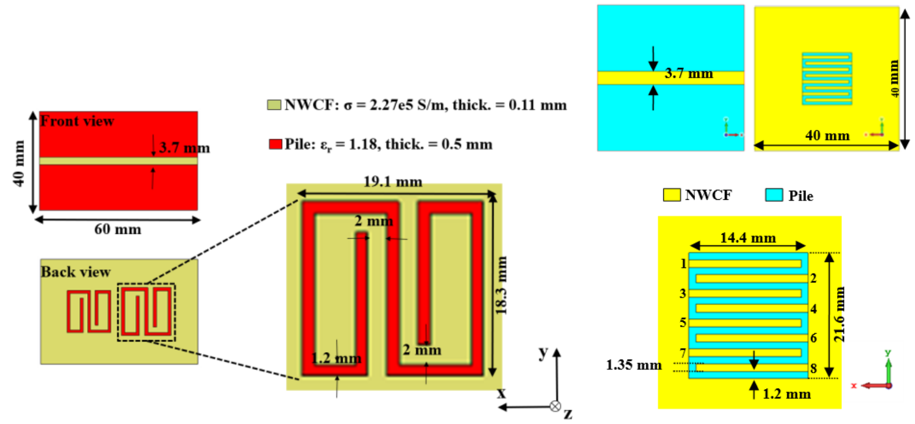

(a) (b)

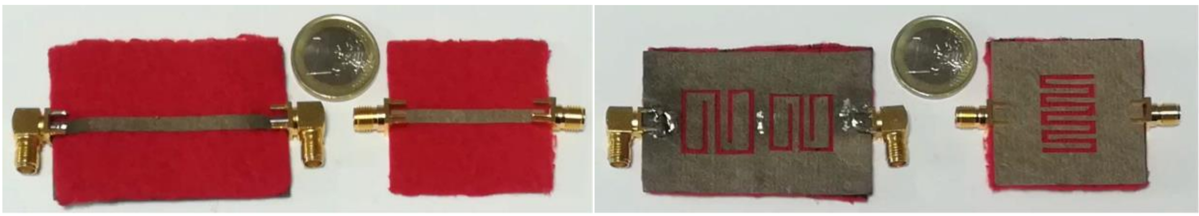

(c) (d)

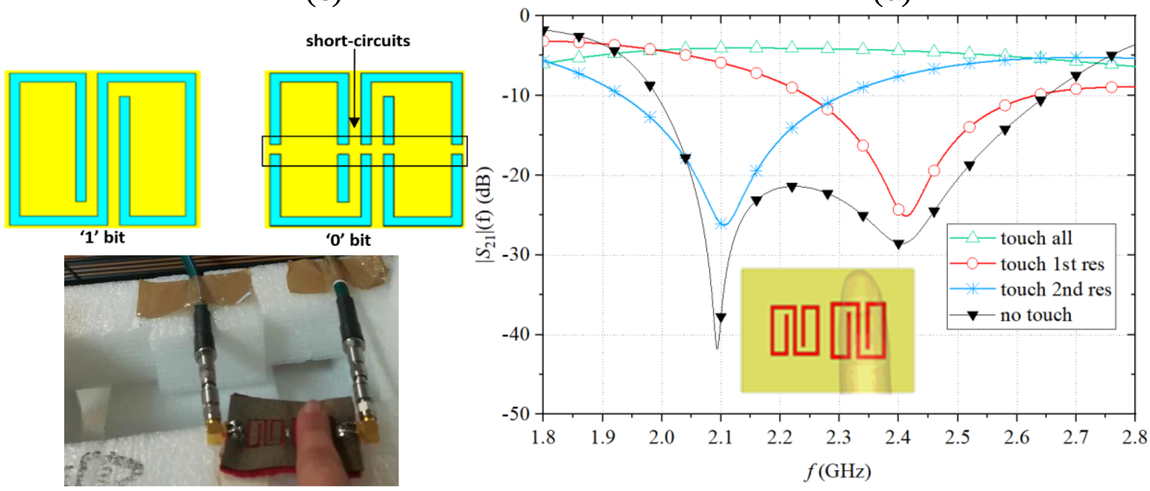

© 2022 IEEE. Personal use of this material is permitted. Permission from IEEE must be obtained for all other uses, in any current or future media, including reprinting/republishing this material for advertising or promotional purposes, creating new collective works, for resale or redistribution to servers or lists, or reuse of any copyrighted component of this work in other works.

(e) (f)

Figure 16: Chipless tags presented in [35]. (a), (b) Geometry of the tags. (c), (d) Front and back view of the fabricated prototypes. (e) How to deactivate the resonators of the tag in (a) and corresponding logic state. (f) Results obtained when using the tag as touch sensor. [35]

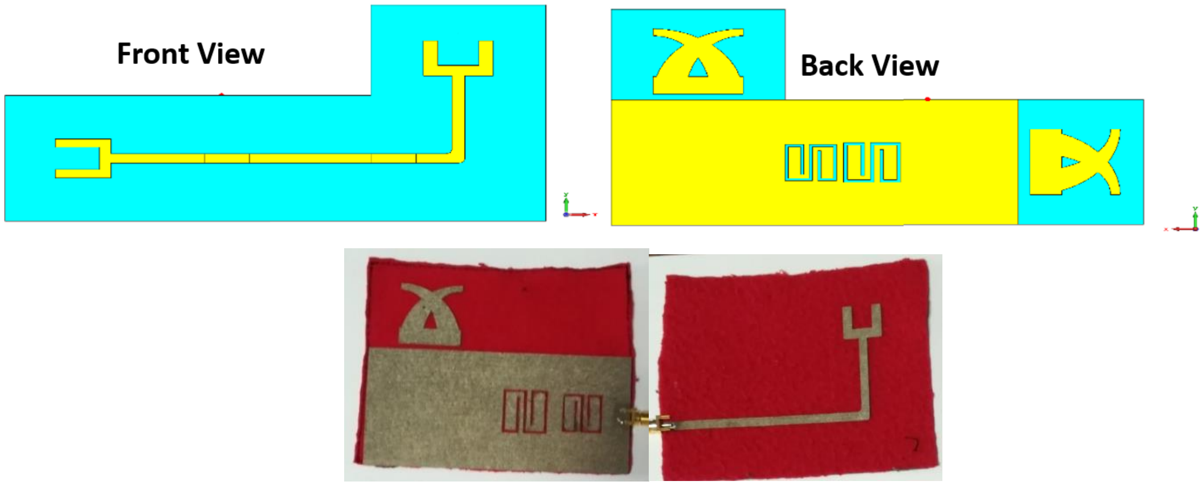

Figure 17. Regarding the wireless connection with the reader, a possible solution for the two cross-polarized antennas has been suggested in [32]. It consists of two microstrip-fed monopoles on a ground plane connected to the tag as illustrated in Fig. 3.

As per the tag illustrated in Fig. 16b it is based on the frequency shift coding technique. It consists of a microstrip line with a hairpin resonator slotted on the ground plane. The hairpin resonator introduces a transmission zero on the transmission coefficient of the microstrip line. When the finger touches the hairpin resonator, as illustrated in Fig. 18, it short-circuits some fingers of the resonator and consequently leads to a frequency shift of the transmission zero. In this case, the position of the finger on the resonator can be recognized by the frequency position of the transmission zero. This behavior is illustrated in Fig. 18.

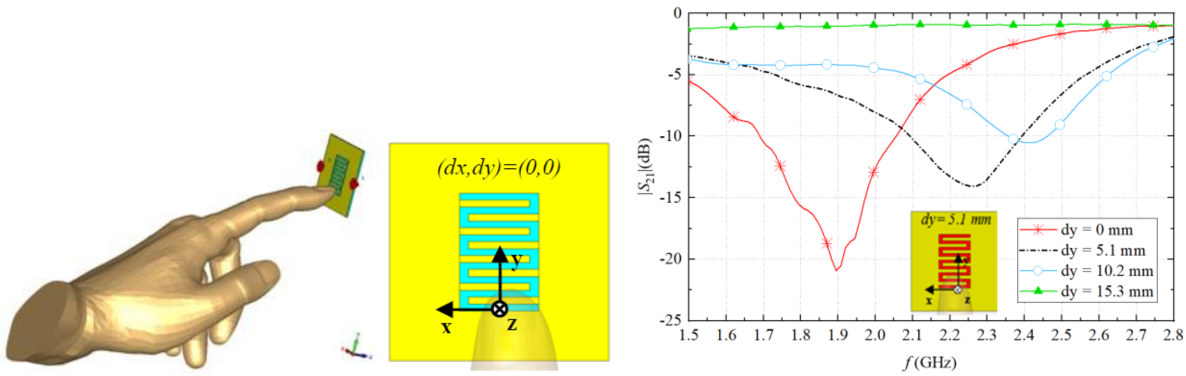

© 2022 IEEE. Personal use of this material is permitted. Permission from IEEE must be obtained for all other uses, in any current or future media, including reprinting/republishing this material for advertising or promotional purposes, creating new collective works, for resale or redistribution to servers or lists, or reuse of any copyrighted component of this work in other works.

Figure 18: Results obtained when using the tag illustrated in Fig. 2b as touch sensor.

In [36] a chipless tag for gesture recognition applications is presented; similarly, to the tags illustrated in Fig. 16, the materials adopted for fabrication are pile as the dielectric substrates (a layer with a thickness of 1 mm has been used) and the NWCF for the conductive parts.
A photograph of the tag applied on a glove is illustrated in Fig. 19a. The tag consists of a stub-loaded microstrip line. The stubs are open-ended quarter-wave resonators with different lengths and are separated from the microstrip line by a small gap.
When the tag is stretched out, the stubs are not electrically connected to the microstrip line and there are no zeros in the transmission coefficients. By bending one of the stubs in such a way that the corresponding stub-line gap is short-circuited, an electrical contact is established between the microstrip line and the stub. At the resonant frequency at which the stub length is equal to $\lambda/4$, the stub behaves as an impedance inverter transforming its open-circuit load into a short-circuit load for the microstrip line, thus leading to the presence of a transmission zero. Accordingly, by positioning the tag on a glove as illustrated in Fig. 19a, the bending of a specific finger can be recognized by the presence/absence of the transmission zero corresponding to that finger.
The results obtained for a three-finger prototype are reported and discussed in [36]; a photograph is given in Fig. 19b. In this prototype the electric contact due to the bending of the fingers is optimized by the presence on the microstrip line of a small fleece cylinder coated with the conductive fabric at the stub positions.

(a) (b)

© 2022 IEEE. Personal use of this material is permitted. Permission from IEEE must be obtained for all other uses, in any current or future media, including reprinting/republishing this material for advertising or promotional purposes, creating new collective works, for resale or redistribution to servers or lists, or reuse of any copyrighted component of this work in other works.

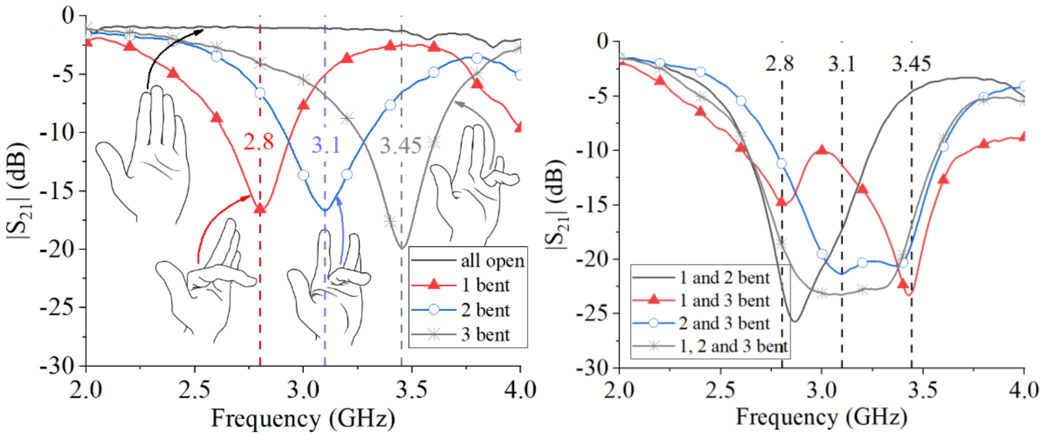

(c)

Fig. 19 : (a) Application of the tag presented in [36] on a glove. (b) Three-finger prototype analyzed in the paper. (c) Experimental results referring to the three-finger prototype [36].

The results obtained for different position of the fingers are illustrated in Fig. 19c. As it can be seen the position of the fingers (bent or straight) can be recognized from the inspection of the transmission coefficient of the microstrip line.
Two planar monopoles suitable to be integrated with the tag for the wireless communication with the reader have been conceived in [36] and are shown in the photo of Fig. 20a positioned on the hand.

According to the retransmission architecture of chipless tags, in order to exploit the device for gesture recognition applications, a reader having two cross-polarized antennas has to be used. In [36] the part of the system relating to the reader (both hardware and processing software) is not developed, but preliminary communication tests are presented. In more detail, experimental tests for evaluating the communication with the reader were performed by integrating one of the two antennas into the tag as a receiving antenna (see Fig. 20a) and using the other as the transmitting one (i.e., as the transmitting antenna of the reader). The achieved results are illustrated in Fig. 20b and refer to a distance between the two antennas of 60 cm. According to these results, a reading distance of the order of a few meters or better is expected with a suitable design of the reader. In fact, for the reader there are no size restrictions, in the final device high gain antennas can be used for the reader side. Additionally, the reading distance can be improved by using a customized post-processing of the received signal.

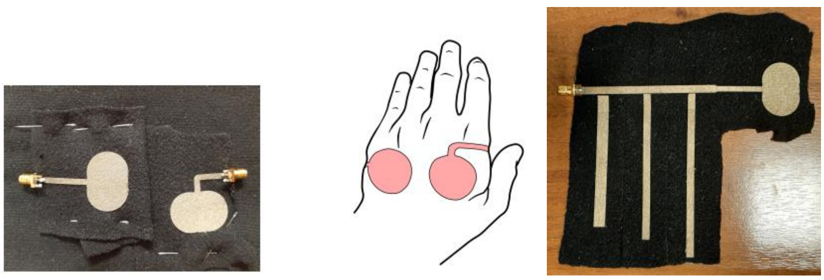

(a)

© 2022 IEEE. Personal use of this material is permitted. Permission from IEEE must be obtained for all other uses, in any current or future media, including reprinting/republishing this material for advertising or promotional purposes, creating new collective works, for resale or redistribution to servers or lists, or reuse of any copyrighted component of this work in other works.

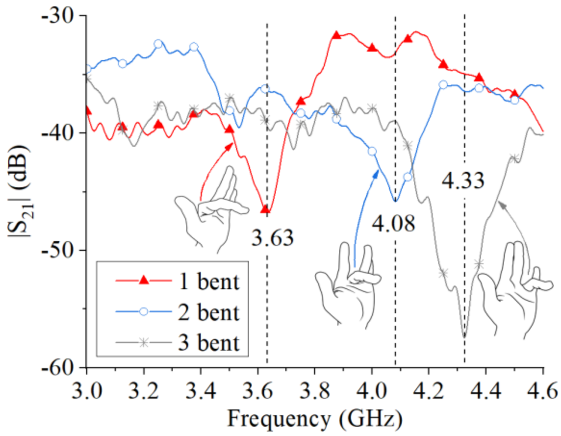

(b)

Figure 20: (a) Antennas proposed in [36] for implementing the wireless communication between the tag and the reader. (b) Results obtained by using one of the antennas illustrated in Fig. 20a integrated with the tag and the other one as transmitting antenna (the measured data refer to a distance between the two antennas of 60 cm).

Embroidered fully-textile tags

Another approach for the fabrication of wearable devices with a high level of integrability in common garments consists in using conductive threads and to embroider the device on common textile materials (cotton, fleece, jeans, etc.).

Two chip-less tags based on this approach have been presented in [37],[38].

In [37] an embroidered tag fabricated by using a silver-coated polyamide conductive fiber (HC12) on a cotton substrate and a commercial embroidery system has been presented. The tag exploits a frequency selective surface consisting of concentric octagonal aperiodic loops (see Fig. 21). A 4-bit tag is obtained by using six concentric octagonal loop resonators. The encoded data bits are obtained by Radar Cross Section (RCS) measurements. Experimental data by placing the tag at a distance of about 1 cm from the human body are reported and analyzed (see Fig. 21) by demonstrating a reading range of 180 cm.

© 2022 IEEE. Personal use of this material is permitted. Permission from IEEE must be obtained for all other uses, in any current or future media, including reprinting/republishing this material for advertising or promotional purposes, creating new collective works, for resale or redistribution to servers or lists, or reuse of any copyrighted component of this work in other works.

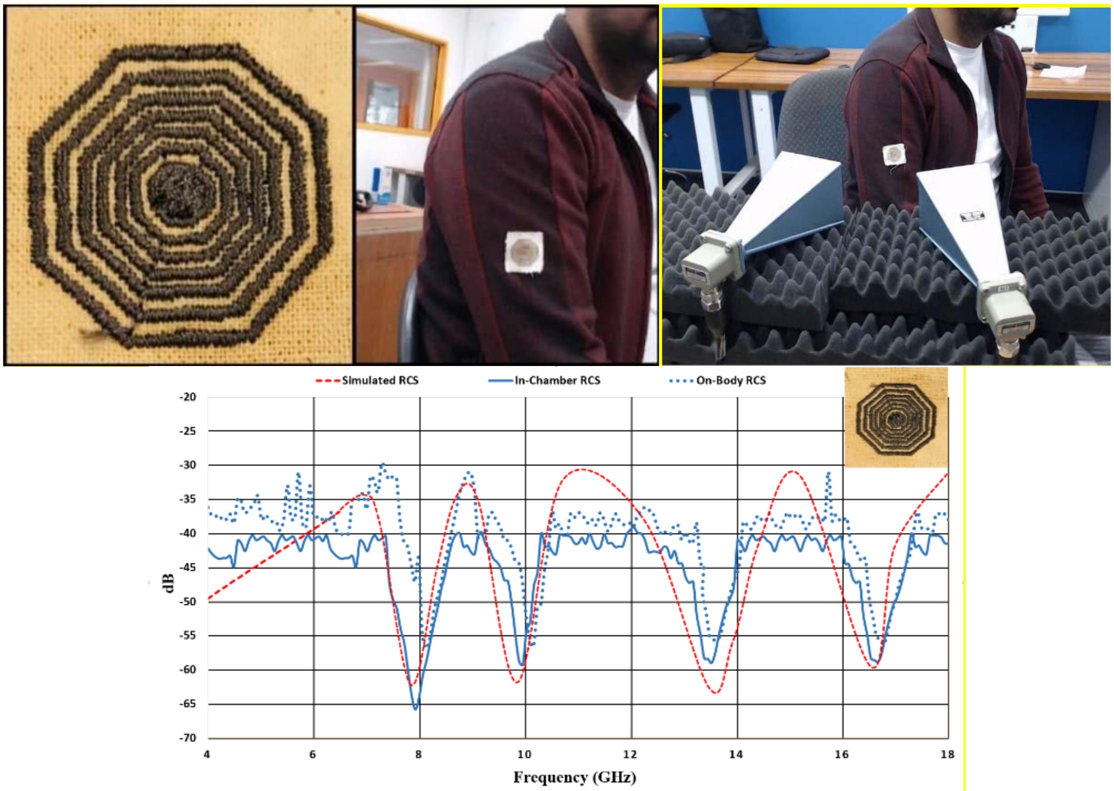

Figure 21: Embroidered tag presented in [37].

In [38] an electro-thread plated with silver is used to embroider three scatters on a cotton textile. In the proposed approach, the presence of a zero in the radar cross section of the tag is related to the presence of a specific resonator. The paper demonstrates the proposed approach for a three scatters device corresponding to a three-bit tag. The results are given in Fig. 22. Measured data reported in Fig. 8 were obtained in un unshielded environment by using a horn antenna for the reader and by placing the tag at a distance of 20 cm from the horn aperture.

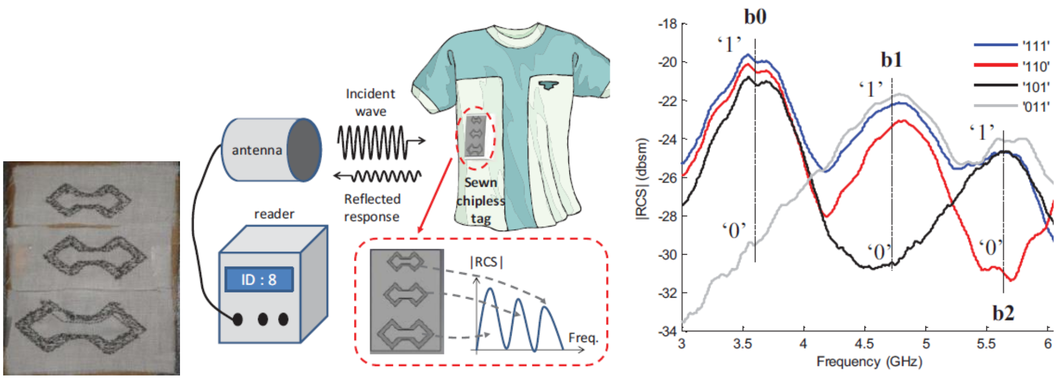

Figure 22: Embroidered tag presented in [38].

Tags on a flexible support

Another approach suitable for obtaining devices that can be applied to the body by adapting to its soft curves consists in using flexible materials as substrate.

© 2022 IEEE. Personal use of this material is permitted. Permission from IEEE must be obtained for all other uses, in any current or future media, including reprinting/republishing this material for advertising or promotional purposes, creating new collective works, for resale or redistribution to servers or lists, or reuse of any copyrighted component of this work in other works.

Based on this approach, a chipless tag for gesture recognition has been presented in [39]. The proposed device exploits resonators which vary their resonant frequency as a function of the induced strain. For obtaining a such behaviour, a stretchable silicone-based electrically conductive adhesive (silo-ECA) was used for the conductive parts of the tag, while a silicone elastomer was used as substrate. In this way a flexible and very thin device is obtained that can be applied on the hand acting like a "smart skin".

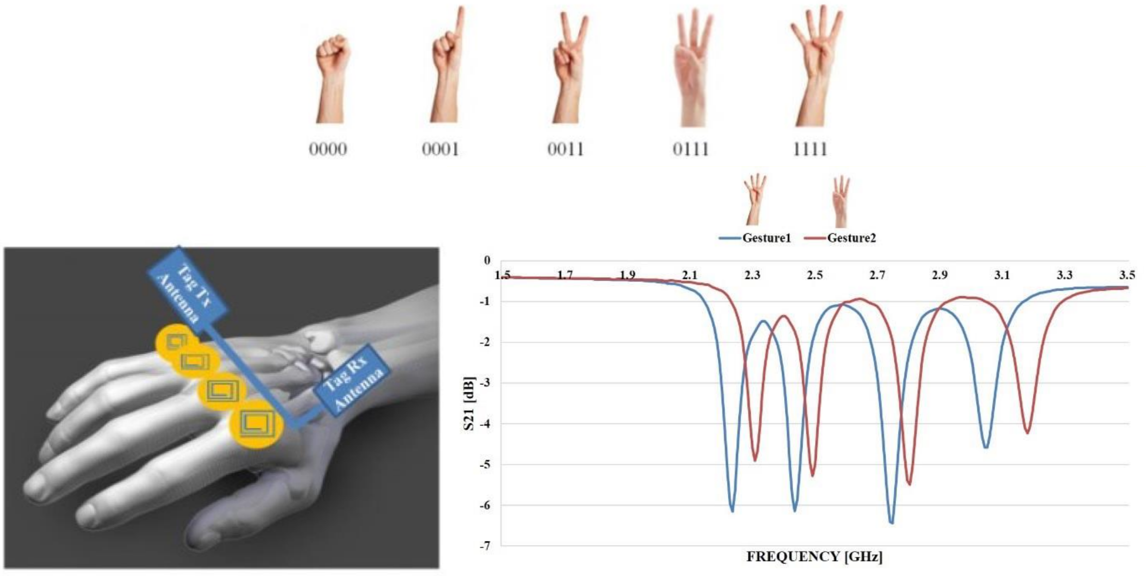

Figure 23: The tag on a stretchable substrate presented in [39].

In [44] a mm-wave chipless sensing sticker has been presented. The proposed tag consists of a Van-Atta reflectarray. In addition to the tag, a high-performance reading system based on polarimetric interrogation, and a time-frequency data processing scheme is also presented and discussed.
The system operate in the Ka-band and a reading range of 30 m is demonstrated.
A photograph of the fabricated tag is illustrated in Fig. 24a, it is inkjet printed by using a silver nanoparticle ink on a low-cost Kapton HN polyimide substrate. In Fig. 24c the setup adopted for measurements is shown, while in Fig. 24d the spectrogram measured for a distance of 30.5 meters is shown.

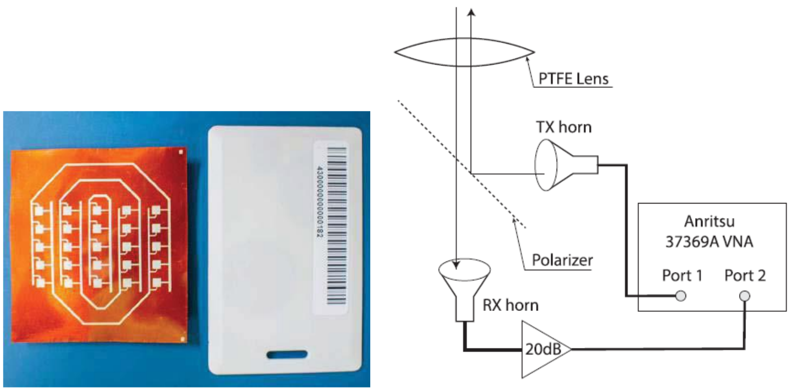

(a) (b)

© 2022 IEEE. Personal use of this material is permitted. Permission from IEEE must be obtained for all other uses, in any current or future media, including reprinting/republishing this material for advertising or promotional purposes, creating new collective works, for resale or redistribution to servers or lists, or reuse of any copyrighted component of this work in other works.

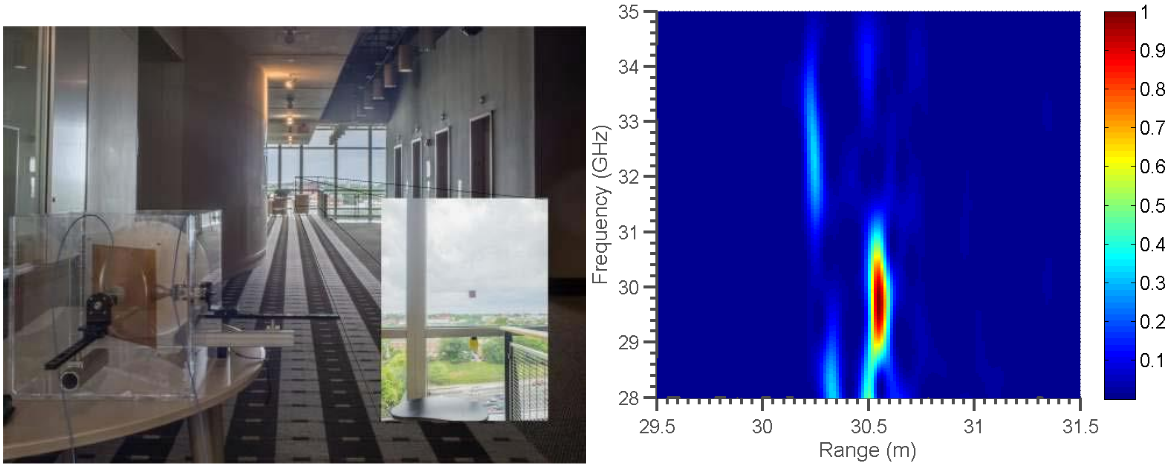

(c) (d)

Figure 24: Tag presented in [44]. (a) Photograph of the tag based on a Van-Atta reflectarray; (b) schematic representation of the reading system based on polarimetric interrogation; (c), (d) measurements setup and measured spectrogram when the reader and the tag are at a distance of 30.5 m.

CONCLUSIONS

This article has reviewed some recent systems whose main feature the energy autonomy is. Several applications have been described subdividing the topic into two categories: energy-harvesting-based systems, embedding the circuit which can store the energy received to self-sustain its operations, and chipless systems whose operations do not rely on an active chip but on the microwave characteristics of their passive circuits layouts and can be fully realized using textiles material and embedded in garments.

These systems can find suitable applications in modern IoT implementations where the need of wearable sensors for multiple purposes, such as localization, remote monitoring of patients, environment quality control is of paramount importance and interest. Indeed energy-autonomy systems allows to avoid the use of batteries as well as the destructive impact on the overall pollution that the disposal of such batteries implies. The energy is provided wirelessly to the receiving wearable tag through electromagnetic waves and either used to power some sensors or backscattered to the source for signal processing, as in the case of the chipless systems.

REFERENCES

[1] L. Corchia, G. Monti, L. Tarricone, “Wearable Antennas: Non-Textile Solutions versus Fully-Textile Solutions," IEEE Antennas and Propagation Magazine, vol. 61, issue 2, 2019.
[2] M. Meyer, Nguyen Van Bình, V. Calero, L. Baraban, G. Cuniberti and J. A. Rogers, "Imperceptible sensorics for medical monitoring," *2015 IEEE 15th International Conference*

© 2022 IEEE. Personal use of this material is permitted. Permission from IEEE must be obtained for all other uses, in any current or future media, including reprinting/republishing this material for advertising or promotional purposes, creating new collective works, for resale or redistribution to servers or lists, or reuse of any copyrighted component of this work in other works.

on Nanotechnology (IEEE-NANO), 2015, pp. 1309-1312, doi: 10.1109/NANO.2015.7388873. MC10
[3] E. M. Amin, J. K. Saha and N. C. Karmakar, "Smart Sensing Materials for Low-Cost Chipless RFID Sensor," in *IEEE Sensors Journal*, vol. 14, no. 7, pp. 2198-2207, July 2014, doi: 10.1109/JSEN.2014.2318056.
[4] C. Occhiuzzi, S. Parrella, F. Camera, S. Nappi and G. Marrocco, "RFID-Based Dual-Chip Epidermal Sensing Platform for Human Skin Monitoring," in *IEEE Sensors Journal*, vol. 21, no. 4, pp. 5359-5367, 15 Feb.15, 2021, doi: 10.1109/JSEN.2020.3031664.
[5] C. -W. Chang, P. Riehl and J. Lin, "Wireless Charging for Smart Garment with Textile-based Receiver Coils," *2020 IEEE Wireless Power Transfer Conference (WPTC)*, 2020, pp. 484-487, doi: 10.1109/WPTC48563.2020.9295550.
[6] J. Antonio Estrada *et al*., "RF-Harvesting Tightly Coupled Rectenna Array Tee-Shirt With Greater Than Octave Bandwidth," in *IEEE Transactions on Microwave Theory and Techniques*, vol. 68, no. 9, pp. 3908-3919, Sept. 2020, doi: 10.1109/TMTT.2020.2988688.
[7] Scavenging for Energy: A Rectenna Design for Wireless Energy Harvesting in UHF Mobile Telephony Bands," in *IEEE Microwave Magazine*, vol. 18.
[8] P. Mezzanotte, V. Palazzi, F. Alimenti and L. Roselli, "Innovative RFID Sensors for Internet of Things Applications," in *IEEE Journal of Microwaves*, vol. 1, no. 1, pp. 55-65, winter 2021, doi: 10.1109/JMW.2020.3035020.
[9] D. Allane, G. Andia Vera, Y. Duroc, R. Touhami and S. Tedjini, "Harmonic Power Harvesting System for Passive RFID Sensor Tags," in *IEEE Transactions on Microwave Theory and Techniques*, vol. 64, no. 7, pp. 2347-2356, July 2016, doi: 10.1109/TMTT.2016.2574990.
[10] H. Solar, A. Beriain, I. Zalbide, E. D'Entremont, and R. Berenguer, "A robust, −40° to +150 °C wireless rotor temperature monitoring system based on a fully passive UHF RFID sensor tag," in IEEE MTT-S Int. Microw. Symp. Dig., Tampa, FL, USA, Jun. 2014, pp. 1–3.
[11] S. Rima, A. Georgiadis, A. Collado, R. Goncalves, and N. Carvalho, "Passive UHF RFID enabled temperature sensor tag on cork substrate," in Proc. IEEE Int. Conf. RFID Technol. Appl., Tampere, Finland, Sep. 2014, pp. 82–85.
[12] A. Faul and J. Naber, "Design and test of a 915 MHz, RFID-based pressure sensor for Glaucoma," in Proc. IEEE 5th Latin Amer. Symp. Circuits Syst., Santiago, Chile, Feb. 2014, pp. 1–4.
[13] S. Mondal and P. Chahal, "A Passive Harmonic RFID Tag and Interrogator Development," in *IEEE Journal of Radio Frequency Identification*, vol. 3, no. 2, pp. 98-107, June 2019, doi: 10.1109/JRFID.2019.2910234.
[14] V. Palazzi, F. Alimenti, C. Kalialakis, P. Mezzanotte, A. Georgiadis and L. Roselli, "Highly Integrable Paper-Based Harmonic Transponder for Low-Power and Long-Range IoT Applications," in *IEEE Antennas and Wireless Propagation Letters*, vol. 16, pp. 3196-3199, 2017, doi: 10.1109/LAWP.2017.2768383.
[15] N. Decarli, F. Guidi and D. Dardari, "Passive UWB RFID for Tag Localization: Architectures and Design," in IEEE Sensors Journal, vol. 16, no. 5, pp. 1385-1397, March1, 2016, doi: 10.1109/JSEN.2015.2497373.

© 2022 IEEE. Personal use of this material is permitted. Permission from IEEE must be obtained for all other uses, in any current or future media, including reprinting/republishing this material for advertising or promotional purposes, creating new collective works, for resale or redistribution to servers or lists, or reuse of any copyrighted component of this work in other works.

[16] D. Dardari *et al*., "An Ultra-Low Power Ultra-Wide Bandwidth Positioning System," in *IEEE Journal of Radio Frequency Identification*, vol. 4, no. 4, pp. 353-364, Dec. 2020, doi: 10.1109/JRFID.2020.3008200.
[17] N. Decarli, M. Del Prete, D. Masotti, D. Dardari and A. Costanzo, "High-Accuracy Localization of Passive Tags With Multisine Excitations," in IEEE Transactions on Microwave Theory and Techniques, vol. 66, no. 12, pp. 5894-5908, Dec. 2018, doi: 10.1109/TMTT.2018.2879806.
[18] N. Pan, D. Belo, M. Rajabi, D. Schreurs, N. B. Carvalho and S. Pollin, "Bandwidth Analysis of RF-DC Converters Under Multisine Excitation," in *IEEE Transactions on Microwave Theory and Techniques*, vol. 66, no. 2, pp. 791-802, Feb. 2018, doi: 10.1109/TMTT.2017.2757473.
[19] Y. -W. Chong, W. Ismail, K. Ko and C. -Y. Lee, "Energy Harvesting For Wearable Devices: A Review," in *IEEE Sensors Journal*, vol. 19, no. 20, pp. 9047-9062, 15 Oct.15, 2019, doi: 10.1109/JSEN.2019.2925638.
[20] Aktas, F., Ceken, C. & Erdemli, Y.E. IoT-Based Healthcare Framework for Biomedical Applications. *J. Med. Biol. Eng.* **38,** 966–979 (2018). https://doi.org/10.1007/s40846-017-0349-7.
[21]] Mandal, S., L. Turicchia, and R. Sarpeshkar. “A Low-Power, Battery-Free Tag for Body Sensor Networks.” Pervasive Computing, IEEE 9.1 (2010): 71-77. © 2010, IEEE.
[22] F. Benassi, G. Paolini, D. Masotti and A. Costanzo, "A Wearable Flexible Energy-Autonomous Filtenna for Ethanol Detection at 2.45 GHz," in *IEEE Transactions on Microwave Theory and Techniques*, doi: 10.1109/TMTT.2021.3074155.
[23] S. K. Behera and N. C. Karmakar, "Wearable Chipless Radio-Frequency Identification Tags for Biomedical Applications: A Review [Antenna Applications Corner]," in *IEEE Antennas and Propagation Magazine*, vol. 62, no. 3, pp. 94-104, June 2020, doi: 10.1109/MAP.2020.2983978.
[24] S. Preradovic and N. C. Karmakar, "Chipless RFID: Bar Code of the Future," in *IEEE Microwave Magazine*, vol. 11, no. 7, pp. 87-97, Dec. 2010, doi: 10.1109/MMM.2010.938571.
[25] L. Corchia, G. Monti, E. De Benedetto, Arpaia, P., Tarricone, L., “Fully-textile, wearable chipless tags for identification and tracking applications,” Sensors 2020, 20(2), 429; https://doi.org/10.3390/s20020429.
[26] S. K. Behera and N. C. Karmakar, "Chipless RFID Printing Technologies: A State of the Art," in IEEE Microwave Magazine, vol. 22, no. 6, pp. 64-81, June 2021, doi: 10.1109/MMM.2021.3064099.
[27] S. K. Behera and N. C. Karmakar, "Chipless RFID Printing Technologies: A State of the Art," in *IEEE Microwave Magazine*, vol. 22, no. 6, pp. 64-81, June 2021, doi: 10.1109/MMM.2021.3064099.
[28] Vena, E. Perret and S. Tedjini, "A Fully Printable Chipless RFID Tag With Detuning Correction Technique," in *IEEE Microwave and Wireless Components Letters*, vol. 22, no. 4, pp. 209-211, April 2012, doi: 10.1109/LMWC.2012.2188785.
[29] M. Bhattacharjee, F. Nikbakhtnasrabadi and R. Dahiya, "Printed Chipless Antenna as Flexible Temperature Sensor," in *IEEE Internet of Things Journal*, vol. 8, no. 6, pp. 5101-5110, 15 March15, 2021, doi: 10.1109/JIOT.2021.3051467

© 2022 IEEE. Personal use of this material is permitted. Permission from IEEE must be obtained for all other uses, in any current or future media, including reprinting/republishing this material for advertising or promotional purposes, creating new collective works, for resale or redistribution to servers or lists, or reuse of any copyrighted component of this work in other works.

[30] J. Aliasgari, M. Forouzandeh and N. Karmakar, "Chipless RFID Readers for Frequency-Coded Tags: Time-Domain or Frequency-Domain?," in *IEEE Journal of Radio Frequency Identification*, vol. 4, no. 2, pp. 146-158, June 2020, doi: 10.1109/JRFID.2020.2982822.
[31] M. Pöpperl, A. Parr, C. Mandel, R. Jakoby and M. Vossiek, "Potential and Practical Limits of Time-Domain Reflectometry Chipless RFID," in *IEEE Transactions on Microwave Theory and Techniques*, vol. 64, no. 9, pp. 2968-2976, Sept. 2016, doi: 10.1109/TMTT.2016.2593722.
[32] L. Corchia, G. Monti and L. Tarricone, "A Fully-Textile Chipless Tag," 2018 48th European Microwave Conference (EuMC), 2018, pp. 977-980, doi: 10.23919/EuMC.2018.8541420.
[33] L. Corchia, G. Monti and L. Tarricone, "Textile Chipless Tag based on Frequency Shift Coding Technique," 2019 49th European Microwave Conference (EuMC), 2019, pp. 500-503, doi: 10.23919/EuMC.2019.8910951.
[34] L. Corchia, G. Monti, E. D. Benedetto and L. Tarricone, "A Chipless Humidity Sensor for Wearable Applications," 2019 IEEE International Conference on RFID Technology and Applications (RFID-TA), 2019, pp. 174-177, doi: 10.1109/RFID-TA.2019.8892048.
[35] L. Corchia, G. Monti, E. De Benedetto and L. Tarricone, "Low-Cost Chipless Sensor Tags for Wearable User Interfaces," in IEEE Sensors Journal, vol. 19, no. 21, pp. 10046-10053, 1 Nov.1, 2019, doi: 10.1109/JSEN.2019.2927823.
[36] G. Monti, G. Porcino and L. Tarricone, "Textile Chipless Tag for Gesture Recognition," in IEEE Sensors Journal, doi: 10.1109/JSEN.2021.3082954.
[37] M. U. A. Khan, R. Raad, J. Foroughi, P. I. Theoharis, S. Liu and J. Masud, "A Silver-Coated Conductive Fibre HC12 Sewed Chipless RFID Tag on Cotton Fabric for Wearable Applications," *2020 IEEE 23rd International Multitopic Conference (INMIC)*, 2020, pp. 1-5, doi: 10.1109/INMIC50486.2020.9318155.
[38] A. Vena;E. Moradi, K. Koski, A. A. Babar, L. Sydänheimo, L. Ukkonen, M. M. Tentzeris, "Design and realization of stretchable sewn chipless RFID tags and sensors for wearable applications," *2013 IEEE International Conference on RFID (RFID)*, 2013, pp. 176-183, doi: 10.1109/RFID.2013.6548152.
[39] T. Le, R. A. Bahr, M. M. Tentzeris, B. Song and C. Wong, "A novel chipless RFID-based stretchable and wearable hand gesture sensor," 2015 European Microwave Conference (EuMC), 2015, pp. 371-374, doi: 10.1109/EuMC.2015.7345777.
[40] L. Corchia, G. Monti, L. Tarricone, “Wearable Antennas: Non-Textile Solutions versus Fully-Textile Solutions," IEEE Antennas and Propagation Magazine, vol. 61, issue 2, 2019.
[41] Laura Corchia, Giuseppina Monti and Luciano Tarricone, “Durability of Wearable Antennas Based on Non-Woven Conductive Fabrics: Experimental Study on Resistance to Washing and Ironing", International Journal of Antennas and Propagation, published by Hindawi, Volume 2018, Article ID 2340293, 8 pages, 2018.
[42] G. Monti, L. Corchia, L. Tarricone, “Fabrication Techniques for Wearable antennas,” in Proc. of 42th European Radar Conference (EuRAD), Nuremberg, pp. 435-438, October 9-11, 2013.
[43] L. Corchia, G. Monti, L. Tarricone, “A Frequency Signature RFID Chipless Tag for Wearable Applications,” Sensors, vol. 19, Issue 3, 2019.

© 2022 IEEE. Personal use of this material is permitted. Permission from IEEE must be obtained for all other uses, in any current or future media, including reprinting/republishing this material for advertising or promotional purposes, creating new collective works, for resale or redistribution to servers or lists, or reuse of any copyrighted component of this work in other works.

[44] J. G. D. Hester and M. M. Tentzeris, "Inkjet-Printed Flexible mm-Wave Van-Atta Reflectarrays: A Solution for Ultralong-Range Dense Multitag and Multisensing Chipless RFID Implementations for IoT Smart Skins," in IEEE Transactions on Microwave Theory and Techniques, vol. 64, no. 12, pp. 4763-4773, Dec. 2016, doi: 10.1109/TMTT.2016.2623790.

© 2022 IEEE. Personal use of this material is permitted. Permission from IEEE must be obtained for all other uses, in any current or future media, including reprinting/republishing this material for advertising or promotional purposes, creating new collective works, for resale or redistribution to servers or lists, or reuse of any copyrighted component of this work in other works.